A SUPER-RESOLUTION ALGORITHM FOR EXTENDED TARGET LOCALIZATION

Jonathan Helland, Michael B. Wakin, Gongguo Tang
Department of Electrical Engineering
Colorado School of Mines, Golden, CO 80401
Email: {jhelland, mwakin, gtang}@mines.edu

***Abstract*—We aim to localize extended targets (i.e. non-point targets) using stepped-frequency (SF) radar measurements from multiple transceivers. In particular, we consider a general signal model with directionally varying target reflectivity that can account for many types of extended target geometries. We localize targets under this signal model using a novel convex relaxation of a tensor atomic norm minimization problem that leverages discrete prolate spheroidal sequences (DPSS's). We test this algorithm on simulated data and show that our proposed method outperforms alternatives for our considered signal model.**

Keywords: Stepped Frequency (SF) radar, extended target localization, atomic norm minimization, blind spectral super-resolution, convex optimization

I. Introduction

Target localization, a fundamental problem in radar signal processing, is a common first step in automatic target recognition and tracking systems. In tracking systems, one might consider a stationary aperture which captures images of potentially many moving targets over time. Alternatively, one might consider localizing stationary targets using a system which synthesizes a large aperture by moving a small aperture over the target scene—such a system is referred to as synthetic aperture radar (SAR). In either of these scenarios, the goal is to localize the moving or stationary targets with a high degree of confidence and precision.

In this paper, we consider stepped-frequency (SF) radar measurements of a near-field scene in which the targets within are stationary. An SF radar aperture illuminates the scene using sinusoids over a wide stepped-frequency band. Such systems are used in through-the-wall target detection where targets of interest are located behind a source of signal clutter. The signal clutter can be mitigated [1]–[3], leaving behind the problem considered in this paper.

In a far-field imaging scenario, targets can be modeled as infinitesimal points and one can discretize the target scene into a grid of spatial pixels and construct a dictionary of prototypical signal returns from each grid location. Target localization then becomes a sparse recovery problem which can be solved by methods like back-projection and Lasso [1], [2].

However, if the targets locations are off-grid or—more generally—if the targets are not effectively modeled as points (a near-field imaging scenario), then these methods are ineffective. In particular, the target return signals are no longer superpositions of a few sinusoids of the type but are instead a composite of multi-band signals. Heuristic approaches to localizing extended targets in spite of the multi-band target returns have been proposed in [3], [4], but the success of these approaches is still fundamentally limited by the discretization of the target scene and hence is subject to basis mismatch [5].

In this work, we propose an algorithm inspired by a trio of recent works on atomic norm minimization for point target localization [6], multi-band signal super-resolution [7], and blind super-resolution [8]. For extended target localization, our method leverages the sparsity over continua expressed by the atomic norm [9] to circumvent the limitations of *a priori* grid discretization inherent in back-projection and Lasso. We demonstrate the efficacy of this approach through numerical experiments with simulated measurements.

II. Notation

$a,\ \boldsymbol{a},\ \boldsymbol{A},\ \boldsymbol{\mathcal{A}}$	scalar, vector, matrix, tensor resp.
$\boldsymbol{A}[:,k],\ \boldsymbol{\mathcal{A}}[:,:,k]$	k-th column, matrix slice resp.
$\top,\ \mathrm{H}$	transpose, conjugate transpose
$\circ$	Hadamard product
$\mathrm{Toep}(\boldsymbol{u})$	Hermitian Toeplitz matrix, first row $\boldsymbol{u}^\top$
$\mathrm{vec}(\cdot)$	vectorization operator
$\lVert\cdot\rVert_{2,1}$	sum of column-wise ℓ_2-norms
$\langle\boldsymbol{\mathcal{A}},\boldsymbol{\mathcal{B}}\rangle$	$\mathrm{vec}(\boldsymbol{\mathcal{B}})^{\mathrm{H}}\mathrm{vec}(\boldsymbol{\mathcal{A}})$
$\langle\cdot,\cdot\rangle_{\mathbb{R}}$	$\mathrm{Re}\left\{\langle\cdot,\cdot\rangle\right\}$

For matrices, the reshaped Khatri-Rao product $\odot$ is the column-wise tensor product: $\boldsymbol{A} = [\boldsymbol{a}_1 \ \cdots \ \boldsymbol{a}_n] \in \mathbb{C}^{m\times n}$ and $\boldsymbol{B} = [\boldsymbol{b}_1 \ \cdots \ \boldsymbol{b}_n] \in \mathbb{C}^{p\times n}$, $\boldsymbol{A}\odot\boldsymbol{B} = \left(\boldsymbol{a}_1\boldsymbol{b}_1^\top \ \cdots \ \boldsymbol{a}_n\boldsymbol{b}_n^\top\right) \in \mathbb{C}^{m\times p\times n}$.

III. Problem Setup

In this section, we provide a mathematical signal model for SF radar measurements of extended targets. To begin, define the index set $[n] := \{1,\cdots,n\}$ for any natural number $n\in\mathbb{N}$. We consider an M-element uniform linear array with transceiver elements that transmit and receive at the same spatial location (from the perspective of the targets). Denote the $m\in[M]$ antenna location as $(x_m^\Delta, y_m^\Delta)\in\mathbb{R}^2$ and suppose that each of the M transceivers receives a stepped-frequency signal composed of N equally spaced frequencies over the band $[F_1,F_N]$ with $F_n := F_0 + (n-1)\Delta F$ for all $n\in[N]$ and $\Delta F := (F_N - F_0)/(N-1)$. We make the simplifying assumption that the transceivers do not receive interference from the other transceivers.

We now describe the imaging field. We consider K-many targets distributed throughout the rectangular region

$$\mathbb{F} := \{(x,y) \in \mathbb{R}^2 \,:\, x_{\min} \le x \le x_{\max},\, y_{\min} \le y \le y_{\max}\}$$

and let $\{\mathbb{T}_k\}_{k\in[K]} \subset \mathbb{F}$ denote the disjoint, connected regions occupied by the K targets. We suppose that the antenna line is parallel to the x-axis and that $y_m^{\triangle} = 0$ for all $m \in [M]$.

The signal received by the m-th antenna is $\boldsymbol{y}[n] := \boldsymbol{z}_m^{\natural}[n] + \boldsymbol{w}_m[n]$, where $\boldsymbol{z}_m^{\natural}$ is the cumulative return from all K extended targets—a multi-band signal defined below—and $\boldsymbol{w}_m$ is additive noise. Before defining the target return signal itself, we introduce some additional notation. Let $\tau_m(x,y)$ be the two-way travel time between the m-th antenna and $(x,y) \in \mathbb{F}$. Under the simplifying assumption that target scattering and refraction is negligible, the two-way travel time can be written as $\tau_m(x,y) = \frac{2}{c}\|(x_m^{\triangle}, y_m^{\triangle}) - (x,y)\|_2$, where c is the speed of light. We also assume that there is no clutter due to walls or the ground present in the target return signals. To compactify our notation, we further define $\theta_m(x,y) := \Delta F \tau_m(x,y)$. We model the m-th extended target return as the following multi-band signal:

$$\begin{aligned}\boldsymbol{z}_m^{\natural}[n] &:= \sum_{k=1}^{K} \int_{\mathbb{T}_k} \sigma_m^{(k)}(x,y)\, e^{-i2\pi F_n \tau_m(x,y)}\, d(x,y) \\ &= \sum_{k=1}^{K} \int_{\tau_m^{\min}(\mathbb{T}_k)}^{\tau_m^{\max}(\mathbb{T}_k)} \sigma_m^{(k)}(\tau)\, e^{-i2\pi F_n \tau}\, d\tau,\end{aligned}$$

where $\sigma_m^{(k)}(\cdot)$ (in a slight abuse of notation) is the directionally dependent reflectivity of the k-th target and $\tau_m^{\max}(\mathbb{T}_k) := \sup\{\tau_m(x,y) \,:\, (x,y) \in \mathbb{T}_k\}$ (similarly using the infimum for $\tau_m^{\min}$). Now, define $\theta_m^{\max}(\mathbb{T}_k) := \Delta F\, \tau_m^{\max}(\mathbb{T}_k)$ (analogously for $\theta_m^{\min}(\mathbb{T}_k)$) and then the **band centers** $\widetilde{\theta}_m^{(k)} := \frac{1}{2}(\theta_m^{\max}(\mathbb{T}_k) + \theta_m^{\min}(\mathbb{T}_k))$ with **half-bandwidths** $W_m^{(k)} := \frac{1}{2}(\theta_m^{\max}(\mathbb{T}_k) - \theta_m^{\min}(\mathbb{T}_k))$. We specifically note that for these band centers, there are spatial locations $(x_{k,m}^{\natural}, y_{k,m}^{\natural}) \in \mathbb{T}_k$ such that $\theta_m(x_{k,m}^{\natural}, y_{k,m}^{\natural}) = \widetilde{\theta}_m^{(k)}$; we refer to these locations as the **target centers**. Note: the target centers are central with respect to the two-way travel times between the m-th sensor and k-th target, not necessarily the target geometry. In our algorithm, we assume only one target center per target. We can now, with another slight abuse of notation for $\sigma_m^{(k)}(\cdot)$, rewrite the target return signal model as

$$\boldsymbol{z}_m^{\natural}[n] = \sum_{k=1}^{K} e^{-i2\pi(n-1)\widetilde{\theta}_m^{(k)}} \int_{-W_m^{(k)}}^{W_m^{(k)}} \sigma_m^{(k)}(\theta)\, e^{-i2\pi(n-1)\theta}\, d\theta.$$

The vector version of this model can be written as

$$\boldsymbol{z}_m^{\natural} = \sum_{k=1}^{K} \boldsymbol{e}_{\widetilde{\theta}_m^{(k)}} \circ \boldsymbol{g}_m^{(k)}, \quad \boldsymbol{g}_m^{(k)} := \int_{-W_m^{(k)}}^{W_m^{(k)}} \sigma_m^{(k)}(\theta)\, \boldsymbol{e}_\theta\, d\theta, \quad (1)$$

where $\boldsymbol{e}_\theta := [1, e^{i2\pi\theta}, \cdots, e^{i2\pi(N-1)\theta}]^{\mathrm{H}}$. Note in particular that $\boldsymbol{g}_m^{(k)}$ is a baseband signal which, when multiplied by $\boldsymbol{e}_{\widetilde{\theta}_m^{(k)}}$, is modulated into the band $[\widetilde{\theta}_m^{(k)} - W_m^{(k)}, \widetilde{\theta}_m^{(k)} + W_m^{(k)}]$.

At each sensor, this signal model matches the general formulation for blind inverse problems defined in [8], where unknown sinusoids undergo pointwise multiplication with a collection of unknown vectors. Following the approach in [8], we will regularize this inverse problem by using a subspace model to represent the unknown waveforms $\boldsymbol{g}_m^{(k)}$. We will also utilize a joint model that accounts for all M sensor measurements simultaneously.

IV. Our Approach

This section describes our algorithmic approach to localizing the extended targets.

A. Discrete Prolate Spheroidal Sequences (DPSS's)

It is well-established [10], [11] that baseband signals of the form $\boldsymbol{g}_m^{(k)}$ are well-approximated using a basis of DPSS's [12], which are time-limited sequences whose DTFT is optimally concentrated (according to the uncertainty principle) within a narrow band. In particular, given a half-bandwidth $W \in (0, 1/2)$, the DPSS's are real, orthonormal, N-dimensional vectors $\boldsymbol{s}_{N,W}^{(\ell)}$ that are spectrally well-concentrated within the baseband $[-W, W]$. Stack these vectors into the matrix $\boldsymbol{S}_{N,W} := [\boldsymbol{s}_{N,W}^{(1)}, \cdots, \boldsymbol{s}_{N,W}^{(L)}] \in \mathbb{R}^{N\times L}$ for some $L \in [N]$. It has been shown [10] that choosing $L = \lceil 2NW(1-\epsilon)\rceil$ for some $\epsilon \in (0,1)$ yields a basis matrix $\boldsymbol{S}_{N,W}$ whose column span very accurately represents W-baseband signals. DPSS's can be computed as the eigenvectors of a certain Toeplitz matrix using implementations in Matlab or SciPy; for more details on computational methods, we refer the reader to [13].

B. The Atomic Dictionary and Norm

By using the approximate subspace model $\boldsymbol{g}_m^{(k)} \approx \boldsymbol{S}_{N,W_m^{(k)}} \boldsymbol{h}_m^{(k)}$ for some $\boldsymbol{h}_m^{(k)} \in \mathbb{C}^{L_m}$, $L_m := \lceil 2NW_m(1-\epsilon)\rceil$ (W_m is defined below) as in Section IV-A, we can build an approximate signal model to (1):

$$\boldsymbol{z}_m^{\natural} \approx \sum_{k=1}^{K} \boldsymbol{e}_{\widetilde{\theta}_m^{(k)}} \circ (\boldsymbol{S}_{N,W_m^{(k)}} \boldsymbol{h}_m^{(k)}).$$

Towards developing our algorithm, we make the assumption that we can accurately represent the $\boldsymbol{g}_m^{(k)}$ for a fixed m using M-many DPSS bases, denoted for each $m \in [M]$ as $\boldsymbol{S}_m := [\boldsymbol{S}_{N,W_m}, \boldsymbol{0}_{N\times(L-L_m)}]$ where $W_m := \max_k(W_m^{(k)})$, $L := \max_m(L_m)$, and $\boldsymbol{0}_{N\times(L-L_m)} \in \mathbb{R}^{N\times(L-L_m)}$ is a matrix of zeros in order to enforce that all $\boldsymbol{S}_m$ have the same dimensions regardless of the individual subspace dimensions L_m. This reduction in DPSS's can be justified by the fact that narrow-band signals can still be well-approximated by a wider-band DPSS basis. If estimates of the W_m are not known in practice, one can further simplify the algorithm by using one DPSS basis by taking $W := \max_m(W_m)$—we demonstrate this flexibility in Section VI. Now, by defining the matrix $\boldsymbol{E}_{(x,y)} := [\boldsymbol{e}_{\theta_1(x,y)}, \cdots, \boldsymbol{e}_{\theta_M(x,y)}]$, we can compactly represent the $N \times M$ collection of all vector measurements from the antenna array as the matrix

$$\boldsymbol{Z}^{\natural} = \sum_{k=1}^{K} \boldsymbol{E}_{(x_k^{\natural}, y_k^{\natural})} \circ \begin{bmatrix} \boldsymbol{S}_1 \boldsymbol{h}_1^{(k)} & \cdots & \boldsymbol{S}_M \boldsymbol{h}_M^{(k)} \end{bmatrix} \quad (2)$$

for some $\boldsymbol{H}_k := [\boldsymbol{h}_1^{(k)}, \cdots, \boldsymbol{h}_M^{(k)}] \in \mathbb{C}^{L\times M}$. Similarly concatenating the measurements and noise into matrices $\boldsymbol{Y}$ and $\boldsymbol{W}$, we have $\boldsymbol{Y} := \boldsymbol{Z}^{\natural} + \boldsymbol{W}$.

Now define the linear measurement operator

$$\mathcal{L}(\boldsymbol{\mathcal{Z}}) := \left[(\boldsymbol{S}_1 \circ \boldsymbol{Z}_1)\mathbf{1}_L \quad \cdots \quad (\boldsymbol{S}_M \circ \boldsymbol{Z}_M)\mathbf{1}_L\right],$$

where the tensor slices $\boldsymbol{Z}_m := \boldsymbol{\mathcal{Z}}[:,:,m] \in \mathbb{C}^{N\times L}$ and $\mathbf{1}_L \in \mathbb{R}^L$ is the vector of all ones. Then we can view the target returns in (2) as $\mathcal{L}$ applied to a K-sparse combination of tensor elements from the continuously parameterized atomic dictionary

$$\mathcal{A} := \{\boldsymbol{\mathcal{A}}(x,y,\boldsymbol{H}) : (x,y) \in \mathbb{F},\ \|\boldsymbol{H}\|_F = 1\}, \tag{3}$$

where $\boldsymbol{\mathcal{A}}(x,y,\boldsymbol{H}) := \boldsymbol{E}_{(x,y)} \odot \boldsymbol{H} \in \mathbb{C}^{N\times M\times L}$. Specifically,

$$\boldsymbol{Z}^\natural = \sum_{k=1}^{K} c_k \mathcal{L}\left(\boldsymbol{\mathcal{A}}(x_k^\natural, y_k^\natural, \boldsymbol{H}_k)\right),$$

where $c_k \in \mathbb{C}$ is a scalar corresponding to the relative dimness of the k-th target i.e. the fact that the unit Frobenius-norm $\boldsymbol{H}_k$ may need re-scaling.

The atomic norm induced by a compact, radially symmetric set $\mathcal{A}$ is defined as

$$\|\boldsymbol{\mathcal{Z}}\|_{\mathcal{A}} := \inf_{\boldsymbol{\mathcal{A}}_k\in\mathcal{A},\ c_k\in\mathbb{C}} \left\{\sum_k |c_k| : \boldsymbol{\mathcal{Z}} = \sum_k c_k \boldsymbol{\mathcal{A}}_k\right\}, \tag{4}$$

which is a gauge function associated with the convex hull of $\mathcal{A}$. Part of our algorithm will require defining the dual atomic norm

$$\|\boldsymbol{P}\|_{\mathcal{A}}^* := \sup_{\|\boldsymbol{\mathcal{Z}}\|_{\mathcal{A}}\le 1} \langle \boldsymbol{P}, \mathcal{L}(\mathcal{Z})\rangle_{\mathbb{R}}. \tag{5}$$

C. Atomic Soft Thresholding (AST)

In order to find an estimate $\widehat{\boldsymbol{Z}}$ from the noisy measurements $\boldsymbol{Y} = \boldsymbol{Z}^\natural + \boldsymbol{W}$ that is a sparse combination of atomic dictionary $\mathcal{A}$ elements, we can solve the Atomic Soft Thresholding (AST) problem

$$\underset{\boldsymbol{\mathcal{Z}}\in\mathbb{C}^{N\times L\times M}}{\text{minimize}}\ \frac{1}{2}\|\boldsymbol{Y} - \mathcal{L}(\boldsymbol{\mathcal{Z}})\|_F^2 + \lambda\|\boldsymbol{\mathcal{Z}}\|_{\mathcal{A}}, \tag{6}$$

where λ is a penalty parameter chosen proportionally to the noise level of $\boldsymbol{W}$ relative to $\boldsymbol{Z}^\natural$. The choice of λ depends precisely on the noise model [14], [15]; we find that if the entries of $\boldsymbol{W}$ are independent copies of a centralized Gaussian random variable with variance ν^2, then a good choice is

$$\lambda = \nu\|\boldsymbol{S}\|_F\left(1 + \frac{1}{\log(NM)}\right) \cdot \sqrt{NM\log(NM) + NM\log(4\pi\log(NM))}.$$

D. Target Localization via the Dual Polynomial

By solving the dual problem to (6), we can expose the atomic structure of $\boldsymbol{Z}^\natural$ and use the dual optimal solution to construct the so-called dual polynomial which localizes the target centers $(x_k^\natural, y_k^\natural)$ (up to a fundamental information limit due to noise). The dual optimal solution $\boldsymbol{\mathcal{P}}^\star \in \mathbb{C}^{N\times L\times M}$ to the Lagrangian dual of (6) can then be used to construct a trigonometric polynomial $q(x,y,\boldsymbol{H}) := |\langle \boldsymbol{\mathcal{P}}^\star, \boldsymbol{\mathcal{A}}(x,y,\boldsymbol{H})\rangle|$, which can be reduced[1] to the $\boldsymbol{H}$-invariant form

$$q(x,y) := \|\Psi_{(x,y)}^*(\boldsymbol{\mathcal{P}}^\star)\|_F, \tag{7}$$

[1]This reduction is not obvious—we omit the derivation due to space constraints.

where

$$\Psi_{(x,y)}^*(\boldsymbol{\mathcal{P}}) := \left[\boldsymbol{P}_1^\top \boldsymbol{e}_{-\theta_1(x,y)} \quad \cdots \quad \boldsymbol{P}_M^\top \boldsymbol{e}_{-\theta_M(x,y)}\right] \in \mathbb{C}^{N\times M}$$

with tensor slices $\boldsymbol{P}_m := \boldsymbol{\mathcal{P}}[:,:,m] \in \mathbb{C}^{N\times L}$. We call $q(x,y)$ the **dual polynomial**, from which estimates of the target centers $(x_k^\natural, y_k^\natural)$ can then be localized from the peaks $\widehat{\Omega} := \{(x,y) : q(x,y) = 1\}$. We refer the reader to [8], [14], [16], [17] for a more in depth discussion of duality theory and the dual polynomial for atomic norm minimization problems. Also see [18] for an overview of atomic norm algorithms in a wide range of contexts.

V. Computation via Semi-Definite Relaxation

This section provides a computational method to solve the AST problem in (6) by forming a Semi-Definite Program (SDP) that approximates the atomic norm $\|\boldsymbol{\mathcal{Z}}\|_{\mathcal{A}}$. We note that our approach is inspired by [6], [8] and is an extension thereof.

The atomic norm itself is approximately equal to the optimal value of the SDP

$$\begin{aligned} &\underset{\boldsymbol{\mathcal{C}},\boldsymbol{U},u_1}{\text{minimize}}\ \frac{1}{2}u_1 + \frac{1}{2}\sum_{m=1}^{M}\operatorname{tr}(\boldsymbol{C}_m) \\ &\text{subject to}\ \begin{bmatrix}\operatorname{Toep}(\boldsymbol{u}_m) & \boldsymbol{Z}_m \\ \boldsymbol{Z}_m^{\mathrm{H}} & \boldsymbol{C}_m\end{bmatrix} \succeq 0,\ \forall m\in[M] \\ &\qquad \boldsymbol{u}_1[1] = \cdots = \boldsymbol{u}_M[1] = u_1, \end{aligned} \tag{8}$$

where $\boldsymbol{\mathcal{Z}} \in \mathbb{C}^{N\times L\times M}$, $\boldsymbol{\mathcal{C}} \in \mathbb{C}^{L\times L\times M}$, $\boldsymbol{U} \in \mathbb{C}^{N\times M}$, $u_1 \in \mathbb{R}$, and $\boldsymbol{Z}_m := \boldsymbol{\mathcal{Z}}[:,:,m]$, $\boldsymbol{C}_m := \boldsymbol{\mathcal{C}}[:,:,m]$, and $\boldsymbol{u}_m := \boldsymbol{U}[:,m]$. The operator $\operatorname{Toep}(\boldsymbol{u}_m)$ is the Hermitian Toeplitz matrix with $\boldsymbol{u}_m$ as the first row. Denoting the optimal value of (8) as $\operatorname{SDP}(\boldsymbol{\mathcal{Z}})$, it can in fact be shown that $\operatorname{SDP}(\boldsymbol{\mathcal{Z}}) \le \|\boldsymbol{\mathcal{Z}}\|_{\mathcal{A}}$ (we omit the proof due to space constraints).

Using the fact that (8) lower bounds the atomic norm, we can approximately rewrite the AST problem (6) as

$$\begin{aligned} &\underset{\boldsymbol{\mathcal{Z}},\boldsymbol{\mathcal{C}},\boldsymbol{U},u_1}{\text{minimize}}\ \frac{1}{2}\|\boldsymbol{Y} - \mathcal{L}(\boldsymbol{\mathcal{Z}})\|_F^2 + \frac{\lambda}{2}\left(u_1 + \sum_m \operatorname{tr}(\boldsymbol{C}_m)\right) \\ &\text{subject to}\ \begin{bmatrix}\operatorname{Toep}(\boldsymbol{u}_m) & \boldsymbol{Z}_m \\ \boldsymbol{Z}_m^{\mathrm{H}} & \boldsymbol{C}_m\end{bmatrix} \succeq 0,\ \forall m\in[M] \\ &\qquad \boldsymbol{u}_1[1] = \cdots = \boldsymbol{u}_M[1] = u_1. \end{aligned} \tag{9}$$

The SDP (9) can be solved using off-the-shelf solvers like SDPT3 [19] in CVX [20]. We construct the dual polynomial from the solution to (9), which is again only approximate.

A. Separated AST

Another heuristic algorithm to approximate (6) is to solve a separate AST problem for each of the M sensors, effectively ignoring all joint structure between the sensor measurements. That is, we can solve

$$\begin{aligned} &\underset{\boldsymbol{Z},\boldsymbol{C},\boldsymbol{u},u_1}{\text{minimize}}\ \frac{1}{2}\|\boldsymbol{y}_m - \mathcal{L}(\boldsymbol{Z})\|_2^2 + \frac{\lambda}{2}\left(\frac{u_1}{M} + \operatorname{tr}(\boldsymbol{C})\right) \\ &\text{subject to}\ \begin{bmatrix}\operatorname{Toep}(\boldsymbol{u}) & \boldsymbol{Z} \\ \boldsymbol{Z}^{\mathrm{H}} & \boldsymbol{C}\end{bmatrix} \succeq 0, \quad \boldsymbol{u}[1] = u_1 \end{aligned} \tag{10}$$

for each $m \in [M]$, where $\boldsymbol{y}_m := \boldsymbol{Y}[:,m]$ and, in a slight abuse of notation, $\mathcal{L}(\boldsymbol{Z}) = (\boldsymbol{S} \circ \boldsymbol{Z})\mathbf{1}_L$. We can then stack the corresponding dual solutions $\boldsymbol{P}_m^\star$ into a tensor $\boldsymbol{\mathcal{P}}^\star$ and construct the dual polynomial (7) as before. This approach will only succeed when each transceiver is able to localize each target within its range.

VI. Simulations

In this section, we provide numerical experiments using synthetic data to support the efficacy of our proposed approach to target localization via the dual polynomial constructed from the solution to (9).

We consider a target field $\mathbb{F} := [-2, 2] \times [2, 7.5]$ (meters) imaged by an $M = 9$ element linear aperture arranged on the x-axis, spaced uniformly over the interval $[-2, 2]$. We simulate $K = 3$ line targets of width 0.4 meters (the average width of a human male) with left endpoints at $(-0.29, 5.38)$, $(1.55, 6.38)$, and $(-1.69, 6.53)$. We generate the target returns, each of which has a spatially varying reflectivity which either increases or decreases (chosen randomly according to a Bernoulli distribution) over $[0.1, 10]$ along the length of each line segment. We compute the DPSS basis for $W = \max_{m,k}(W_m^{(k)})$ and take the M-many DPSS's as $\boldsymbol{S}_m = \boldsymbol{S}_{N,W}$ for all $m \in [M]$. That is, we only use one DPSS matrix rather than M separate DPSS matrices in order to test the quality of our approximations. A stepped frequency signal consisting of $N = 70$ frequencies spaced uniformly over $[1, 3]$ (GHz) is used to illuminate the scene. Finally, we generate additive measurement noise $\boldsymbol{W}$ according to a complex normal distribution $\mathcal{CN}(0, 0.01^2)$ where the entries of $\boldsymbol{W}$ are independent copies. We again emphasize that in our simulations, we assume that no scattering or clutter is present in the target return signals.

We compare the performance of the back-projection method, AST under the assumption of point targets [6], the Separated AST heuristic (10), and finally our proposed extended target AST method (9). We solve the AST-based methods using CVX equipped with SDPT3. We discretize the target field $\mathbb{F}$ so that each pixel has a spacing of 0.01—that is, a grid of 401×551 pixels over which we evaluate the dual polynomials constructed by each method. To localize the peaks of the dual polynomials, we consider only the points (x, y) for which $q(x, y)$ is near 1 and then use K-means[2] to identify clusters (i.e. peak areas). We then take the (x, y) for which $q(x, y)$ is maximized within the k-th cluster as our estimate of $(x_k^\natural, y_k^\natural)$, repeating for all $k \in [K]$. Figure 1 shows the dual polynomials computed by applying the previously mentioned algorithms to our synthetic measurements (note: the dual polynomial shapes are **not** expected to directly correspond to the target geometries $\mathbb{T}_k$). We can see in Figure 1(d) that our proposed method outperforms the other considered methods—all other dual polynomials have many spurious peaks. It is worth noting that (10) can be a useful heuristic in practice but will, loosely speaking, fail when one sensor fails; (9) has joint structure that prevents this issue.

We emphasize that our algorithm works well despite several levels of approximation: first, the simulated target returns are only approximated by our DPSS signal model (2). Second, we only use one DPSS matrix $\boldsymbol{S}_{N,W}$ by taking

[2]We assume that K is known *a priori* for the sake of algorithm comparison—K can be easily estimated in practice, however, using the Within Cluster Sum of Squares metric.

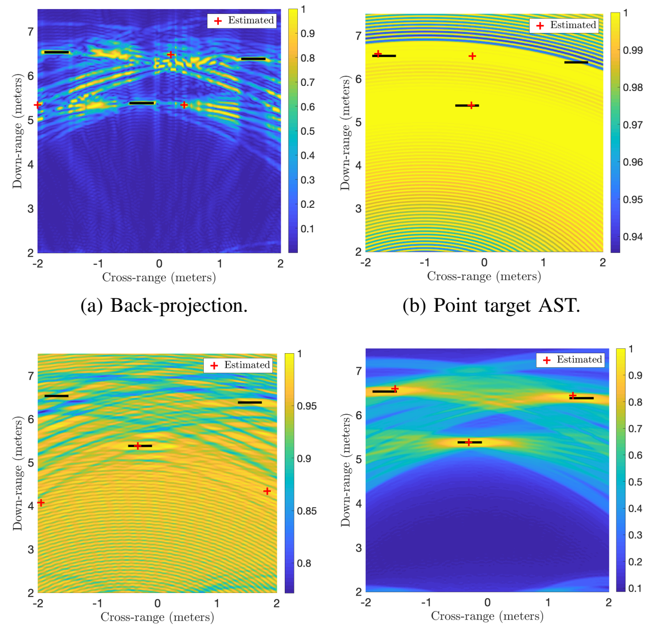

(a) Back-projection. (b) Point target AST.

(c) Separated AST. (d) Proposed method.

Fig. 1: Target localization results using different methods. The targets are the black lines. The spatially parameterized dual polynomials are visualized by the colors. We emphasize that the shapes of the dual polynomials are **not** expected to directly correspond to the geometry of the targets $\mathbb{T}_k$.

$W = \max_{m,k}(W_m^{(k)})$ rather than using M-many $\boldsymbol{S}_m$ (which is itself an approximation since there are KM DPSS matrices present in our approximate signal model (2)) as in the most general formulation of our algorithm.

VII. Conclusion

Using the framework of the atomic norm, we have developed an algorithm for denoising signals resulting from SF radar measurements of extended targets with directionally varying reflectivities that can also localize extended targets in the imaging field. We derived an approximately equivalent SDP (9) for the atomic norm and demonstrated its efficacy in the proposed AST problem using numerical simulations with synthetic SF measurements. Through these experiments, we have demonstrated that this algorithm outperforms alternative algorithms one might consider for this problem using simulated line targets with measurement noise. Lastly, unlike conventional algorithms such as back-projection—which dicretize the frequency domain prior to optimization—our algorithm optimizes over a continuous domain and hence circumvents discretization problems such as off-grid target locations.

Acknowledgment

This work was supported by NSF grants CCF–1409261 and CCF–1704204.

REFERENCES

[1] E. Lagunas, M. G. Amin, F. Ahmad, and M. Nájar, "Joint wall mitigation and compressive sensing for indoor image reconstruction," *IEEE Transactions on Geoscience and Remote Sensing*, vol. 51, no. 2, pp. 891–906, 2012.

[2] F. Ahmad, J. Qian, and M. G. Amin, "Wall clutter mitigation using discrete prolate spheroidal sequences for sparse reconstruction of indoor stationary scenes," *IEEE Transactions on Geoscience and Remote Sensing*, vol. 53, no. 3, pp. 1549–1557, 2014.

[3] Z. Zhu and M. B. Wakin, "Wall clutter mitigation and target detection using discrete prolate spheroidal sequences," in *2015 3rd International Workshop on Compressed Sensing Theory and its Applications to Radar, Sonar and Remote Sensing (CoSeRa)*. IEEE, 2015, pp. 41–45.

[4] ——, "Detection of stationary targets using discrete prolate spheroidal sequences," in *2015 31st International Review of Progress in Applied Computational Electromagnetics (ACES)*. IEEE, 2015, pp. 1–2.

[5] Y. Chi, L. L. Scharf, A. Pezeshki, and A. R. Calderbank, "Sensitivity to basis mismatch in compressed sensing," *IEEE Transactions on Signal Processing*, vol. 59, no. 5, pp. 2182–2195, 2011.

[6] Z. Zhu, G. Tang, P. Setlur, S. Gogineni, M. B. Wakin, and M. Rangaswamy, "Super-resolution in SAR imaging: Analysis with the atomic norm," in *2016 IEEE Sensor Array and Multichannel Signal Processing Workshop (SAM)*. IEEE, 2016, pp. 1–5.

[7] Z. Zhu, D. Yang, M. B. Wakin, and G. Tang, "A super-resolution algorithm for multiband signal identification," in *2017 51st Asilomar Conference on Signals, Systems, and Computers*. IEEE, 2017, pp. 323–327.

[8] D. Yang, G. Tang, and M. B. Wakin, "Super-resolution of complex exponentials from modulations with unknown waveforms," *IEEE Transactions on Information Theory*, vol. 62, no. 10, pp. 5809–5830, 2016.

[9] V. Chandrasekaran, B. Recht, P. A. Parrilo, and A. S. Willsky, "The convex geometry of linear inverse problems," *Foundations of Computational mathematics*, vol. 12, no. 6, pp. 805–849, 2012.

[10] M. A. Davenport and M. B. Wakin, "Compressive sensing of analog signals using discrete prolate spheroidal sequences," *Applied and Computational Harmonic Analysis*, vol. 33, no. 3, pp. 438–472, 2012.

[11] Z. Zhu and M. B. Wakin, "Approximating sampled sinusoids and multiband signals using multiband modulated DPSS dictionaries," *Journal of Fourier Analysis and Applications*, vol. 23, no. 6, pp. 1263–1310, 2017.

[12] D. Slepian, "Prolate spheroidal wave functions, fourier analysis, and uncertainty—v: The discrete case," *Bell System Technical Journal*, vol. 57, no. 5, pp. 1371–1430, 1978.

[13] S. Karnik, Z. Zhu, M. B. Wakin, J. Romberg, and M. A. Davenport, "The fast slepian transform," *Applied and Computational Harmonic Analysis*, 2017.

[14] B. N. Bhaskar, G. Tang, and B. Recht, "Atomic norm denoising with applications to line spectral estimation," *IEEE Transactions on Signal Processing*, vol. 61, no. 23, pp. 5987–5999, 2013.

[15] S. Li, M. B. Wakin, and G. Tang, "Atomic norm denoising for complex exponentials with unknown waveform modulations," *arXiv preprint arXiv:1902.05238*, 2019.

[16] G. Tang, B. N. Bhaskar, P. Shah, and B. Recht, "Compressed sensing off the grid," *IEEE transactions on information theory*, vol. 59, no. 11, pp. 7465–7490, 2013.

[17] Z. Yang and L. Xie, "Exact joint sparse frequency recovery via optimization methods," *IEEE Transactions on Signal Processing*, vol. 64, no. 19, pp. 5145–5157.

[18] Y. Chi and M. F. Da Costa, "Harnessing sparsity over the continuum: Atomic norm minimization for super-resolution," *arXiv preprint arXiv:1904.04283*, 2019.

[19] K.-C. Toh, M. J. Todd, and R. H. Tütüncü, "SDPT3—a MATLAB software package for semidefinite programming, version 1.3," *Optimization Methods and Software*, vol. 11, no. 1-4, pp. 545–581, 1999.

[20] M. Grant and S. Boyd, "CVX: MATLAB software for disciplined convex programming, version 2.1."